文章编号 1004-924X(2011)02-00228-09

半导体量子点材料在 Nd：YAG 激光辐照下的非线性光学效应

KUMBHAKAR P
(Nanoscience Laboratory, Department of Physics,
National Institute of Technology, Durgapur 713209, India)

摘要：使用 10 ns 脉冲调 Q Nd：YAG 激光器 Z-scan 技术测量了化学合成的无掺杂硫化锌量子点(QDs)以及掺 Mn^{2+} 硫化锌量子点(QDs)的非线性光学特性，并使用透射电镜技术(TEM)以及 X 射线衍射法(XRD)表征合成材料的纳米结构。在室温下，分别利用 UV-VIS 分光光度计和分光荧光计测量了人工合成 QDs 胶体溶液的线性光学吸收特性以及光致发光的发射特性。样品的吸收特性表明，由于量子限制效应的影响，样品的截止吸收低于硫化锌的截止吸收。样品的光致发光特性显示，掺 Mn^{2+} 的硫化锌样品显示出明显的光致发光现象，发射峰大约在 580 nm；而无掺杂的硫化锌样品在紫外区辐射，发射峰大约在 365 nm。对样品的 UV-VIS 吸收特性分析和 TEMXRD 分析表明，硫化锌样品的平均粒度(半径)大约为 1.2 nm。分析开放光圈(OA)Z-scan 技术得到的实验数据，发现在 1 064 nm 处两种试验样品都会发生四光子吸收(FPA)现象。拟合实验数据得到了两种试验样品的 FPA 系数以及 FPA 横截面，结果表明，ZnS QD 的 FPA 横截面的计算值是 4.9×10^{-106} $cm^8\cdot s^3\cdot photon^{-3}$，比硫化锌的 FPA 横截面大了 5 个数量级，而且人工合成的 ZnS QD 也有光学限制的性质。掺 Mn^{2+} 离子的样品具有大的 FPA 横截面和在可见光区有高的发光效率这两个特点，使得该材料适合用于多光子荧光成像。

关 键 词：半导体材料；ZnS 量子点；非线性光学特性；多光子吸收；ZnS 掺杂；Mn 掺杂
中图分类号：TN304.2 **文献标识码**：A **doi**：10.3788/OPE.20111902.0228

Observation of nonlinear optical effects in some semiconductor quantum dot materials using Nd：YAG laser radiation

KUMBHAKAR P

(*Nanoscience Laboratory*, *Department of Physics*,
National Institute of Technology, *Durgapur* 713209, *India*)

Abstract: Nonlinear optical (NLO) properties of the colloidal solutions of chemically synthesized undoped and Mn^{2+} doped ZnS Quantum Dots (QDs) in methanol are measured by using a Q-switched 10 ns pulsed Nd：YAG laser radiation by the Z-scan technique. The nanostructures of the synthesized materials are characterized by using different characterization tools, such as Transmission Electron Microscopy (TEM) and X-ray Diffraction (XRD) analysis. Linear optical absorption and Photoluminescence (PL) emission characteristics of the colloidal solutions of the synthesized QDs are measured

收稿日期：2010-10-08；**修订日期**：2010-10-30.
基金项目：DST (Grant No. SR/FTP/PS-67/2008), Govt. of India

at room temperature by using a UV-visible spectrophotometer and a spectrofluorimeter, respectively. The absorption characteristics of the samples show that the absorption cut-off of the samples is below that of the bulk ZnS due to the quantum confinement effect. Photoluminescence emission characteristics measured at room temperature show that the Mn^{2+} doped ZnS sample exhibits its visible PL emission peak at ~580 nm, whereas the undoped ZnS sample emits in the ultraviolet region peak at ~365 nm. The average particle size (radius) of the as-prepared ZnS sample is ~1.2 nm as determined from the measured UV-visible absorption characteristics as well as from TEM and XRD data analyses. By analyzing the experimental data obtained by the Open Aperture (OA) *Z*-scan technique, it is found that the Four-photon Absorption (FPA) takes place at 1064 nm wavelength in both the studied samples. FPA coefficients and FPA cross-section of both the samples are extracted by fitting the experimental data with the available analytical expression. It is found that the calculated value of FPA cross section of ZnS QD is 4.9×10^{-106} $cm^8 \cdot s^3 \cdot photon^{-3}$, which is five orders of magnitude larger than that of bulk ZnS. Optical limiting property of the synthesized ZnS QD is also presented. The simultaneous presence of large FPA cross section and large luminescence efficiency in the visible region in Mn^{2+} doped sample would render this material as a good candidate for multiphoton fluorescence imaging applications.

Key words: semiconductor material; ZnS Quantum dots; nonlinear optical properties; multiphoton absorption; ZnS doping; Mn doping

1 Introduction

A lot of attention have been given recently in the synthesis and characterization of semiconductor Quantum Dots (QDs) having dimensions comparable to the Bohr exciton radius (aexc) of its bulk counterpart[1-4]. In such semiconductor QDs, quantum confinement effect plays a major role in determining its optical, electronic and Nonlinear Optical (NLO) properties[1-6] and its optical absorption and Photoluminescence (PL) emission properties can be tuned by tuning the size of the synthesized QDs. The possibility of tailoring the bulk material properties by varying the size, structure, and composition of constituting nanoscale particles makes them candidates for various important applications in the field of material research[3]. Therefore, lots of interest have been given recently to synthesize wide band gap II-VI semiconductors, like ZnS, ZnO, CdS, CdSe, *etc*. with the size of the particles lying within the quantum confinement regime[3-4,7]. Also by doping suitable elements in such semiconductor materials, it is possible to achieve tunable and efficient PL emission in the visible wavelength region. There are various reports for the synthesis of undoped and doped semiconductor QDs by using different synthesis procedure, out of them chemical precipitation method is simple and low cost and so it is suitable for industrial synthesis of semiconductor QDs[3-4].

Out of various II-VI semiconductor materials, ZnS and Mn^{2+} doped ZnS QDs having wide bandgap and large exciton binding energy show prospects for their applications in various optoelectronic devices as visible luminescent materials, as a suitable material for multiphoton imaging applications in medical sciences, and as nonlinear optical materials to be used in various communication networks *etc*.[5-7]. The optical properties of these materials are currently the subject of tremendous investigations, in response to the industrial demand for optoelectronic devices that could operate at short wavelengths. There is a significant demand for materials with higher nonlinearity, which can be integrated into an optoelectronic device.

There are different methods, such as degenerate four-wave mixing, nonlinear interferometry, and the *Z*-scan technique for the measurement of NLO properties of semiconductor materials[8-9]. Among all these methods for investigating the NLO parameters of materials, the most sensitive, easy and informative is the *Z*-scan technique and also it allows the determination of both the value and the sign of the NLO parameters of the investigating materials. The *Z*-scan method proposed by Sheik-Bahae *et al*. [8] has been widely used to determine the NLO characteristics, especially nonlinear refraction and nonlinear absorption of a medium. The measurement of the NLO properties of materials is an important issue of optical science because it allows the determination of their area of applicability to laser physics and optoelectronics. Indeed, for applications of materials as optical limiters or as optical switches, for instance, it is necessary to know their NLO parameters such as the nonlinear absorption (NLA) coefficient and nonlinear refraction (NLR) coefficient. Knowledge of not only the magnitude of these parameters but also their sign is relevant for technological applications. However, there are only few reports on the NLO properties of the bulk ZnS as well as that of undoped and Mn^{2+} doped ZnS QDs[7,9-14].

We have reported the nonlinear optical properties of the chemically synthesized ZnS and Mn^{2+} doped ZnS QDs by *Z*-scan technique. The particle size (radius) of the synthesized semiconductor QDs lies within 1－1.5 nm, which have been estimated by various methods, namely by X-ray diffraction (XRD) analysis, transmission electron microscopy (TEM), and UV-visible optical absorption analysis. The compositional analyses have been done by energy-dispersive X-ray analysis (EDXA) attached with a scanning electron microscope (SEM). Photoluminescence (PL) emission characteristics of the undoped and doped ZnS samples are also measured at room temperature and obtained visible PL emission in the Mn doped sample, whereas the undoped sample emits in the UV region. The NLO properties of ZnS and Mn^{2+} doped ZnS QDs have been investigated by using the *Z*-scan technique and by using the *Q*-switched 10 ns pulsed 1 064 nm Nd:YAG laser wavelength. As the bandgap of the investigated QDs are more than 3.7 eV (bandgap of bulk ZnS) which are much larger than the photon energy of 1.17 eV of the used Nd:YAG laser radiation, nonlinear absorptions in the colloidal solutions of the used QDs samples occurred at the used high intensity of 2.5 GW/cm^2 due to multiphoton absorptions in the samples. By fitting the experimental open aperture (OA) and *Z*-scan transmission trace with the available analytical expression, Four-photon Absorption (FPA) is found to be the dominant mechanism for NLA in the investigated samples and FPA coefficient of the used QDs have been estimated. Also the optical limiting properties of the investigated colloidal solutions of the QDs are presented at 1 064 nm.

2 Experimental Methods

Undoped ZnS and (2.5%) Mn^{2+} doped ZnS QDs are freshly prepared at room temperature by using the same chemical precipitation method as described elsewhere[4]. Here we present briefly the synthesis procedure. All the chemicals used are of AR grade (Merck and SD fine chemicals), used without further purification. Freshly prepared aqueous solutions of the chemicals are used for the synthesis of nanoparticles at room temperature. At first, 10 ml each of both zinc nitrate solution and saturated solution of sodium sulfide in methanol are prepared. Zinc nitrate solution is first vigorously stirred using a magnetic stirrer up to 1 h, and then the solution of sodium sulfide is mixed with the solution of zinc nitrate drop wise up to pH 8. The precipitate is separated from the reaction mixture by centrifu-

gation (Eltek Refrigerated Centrifuge RC 4 100D) for 5 min at 10,000 r/min and is washed several times with methanol to remove all sodium particles. The wet precipitate is then dried up for further measurement and analyses. Mn^{2+}-doped-ZnS nanoparticles are prepared at room temperature of 20 ℃ by mixing calculated amounts of zinc nitrate solution in methanol and manganese acetate solution in methanol followed by drop wise addition of saturated solution of sodium sulfide in methanol up to pH 8. The mixture is vigorously stirred using a magnetic stirrer up to 1 h and the white precipitate is separated from the reaction mixture by centrifugation for 5 min at 10,000 r/min and it is washed several times with methanol to remove all sodium particles and finally dried up for using in the next experiments.

The synthesized samples are characterized for their optical and nanostructural properties. The XRD pattern is recorded with an X-ray diffractometer (PANLYTICAL) using Cu K_α radiation of wavelength 0.154 06 nm in the scan range (2θ) 20 — 75°. The formations of nanostructures are confirmed by TEM (JEOL 2000 FX 11) micrograph. Scanning electron microscope (SEM with EDXA, Sirion) has been used for compositional analysis of the prepared samples. The optical transmission spectra of the samples are recorded using a UV-visible spectrophotometer (Hitachi U-3010) and the PL spectrum of the QDs dispersed in methanol has been measured using a spectrofluorimeter (LS-55, PerkinElmer).

Nonlinear optical properties of the samples are measured using a home built Zscan set up[7-8]. The used experimental arrangement for NLO studies is a standard Z-scan set up and it is shown in Fig. 1. A Q-switched Nd: YAG laser having pulse width of 10 ns delivers a Gaussian beam of 1 064 nm radiation at 10 Hz repetition rate. A part of the incident laser beam is reflected by a beam splitter to enable monitoring of any fluctuation in input energy by continual measurement of the energy of this reflected part. Two detectors (Detector 1 and Detector 2) are used for measurement of the energies of the transmitted and the reflected laser radiations. The transmitted main laser beam is focused by a lens (f = 20 cm). The beam waist and the confocal parameter (z_o) at the focus are thus respectively 67 μm and 1.35 cm. Initially Z-scan data are collected with only methanol. Neither NLR and NLA nor optical damage at the wall of the cuvette has been observed when the maximum value of peak intensity is 2.5 GW/cm^2 on focus. The samples are then dispersed in methanol and kept in a quartz cuvette of optical path length (L) of 2 mm for Z-scan measurement. This satisfies the "thin sample" approximation (*i.e.* $L < z_o$) quite effectively. The cuvette is mounted in a translation stage to move the sample in the pre-focal and post-focal directions along the direction of propagation (z-axis) of the used laser beam. All the Z-scan measurements are carried out at room temperature.

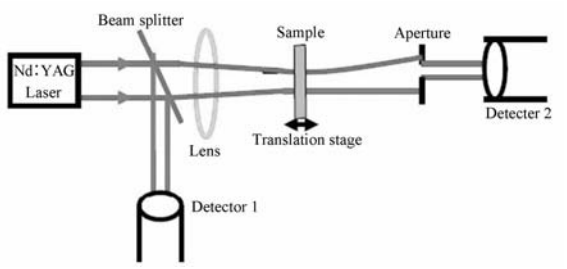

Fig. 1　Experimental arrangement for NLO studies (a standard Z-scan set up)

3　Results and discussions

Fig. 2(a), 2(b), and 2(c) show the XRD pattern of cubic bulk ZnS (as per JCPDS No. 80-020), undoped ZnS, and Mn^{2+} doped ZnS samples, respectively. From the Figs. 2(a), 2(b), and 2(c) it is seen that three diffraction peaks which are appeared at 2θ values of 28.6°, 47.9°, and 56.5° in the synthesized ZnS sample are

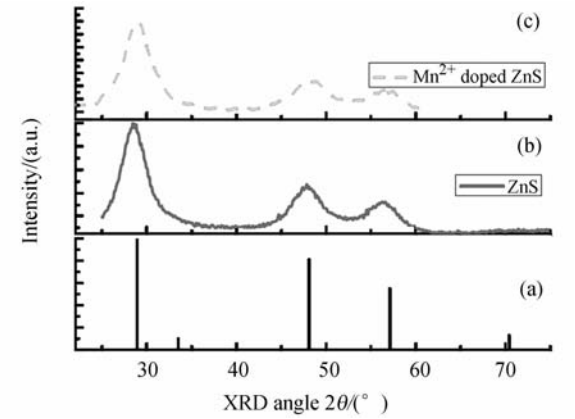

Fig. 2　XRD pattern of cubic bulk ZnS, undoped ZnS, and Mn^{2+} doped ZnS samples

close to the diffraction peaks appeared in standard cubic (zinc blend) phase of ZnS. In the Mn^{2+} doped ZnS sample also these three XRD peaks appeared at 2θ values of 29.0°, 48.2°, and 56.5°, in almost the same positions as those of ZnS sample. These three major peaks are appearing in the XRD pattern of both the samples due to reflections from the (111), (220), and (311) planes of cubic (zinc blend) phase of ZnS[4]. The broadening of the XRD pattern takes place due to the reduction of the particle sizes of the synthesized QDs. The particle size(radius,R) of the synthesized QDs are calculated from the XRD pattern and by using the Debye-Scherer formula[15]:

$$R=\frac{0.89\lambda}{2\beta\cos\theta}. \tag{1}$$

Here, λ is the X-ray wavelength, β is the full-width at half maximum (FWHM) of diffraction peak and θ is the diffraction angle. The calculated particle size as obtained from the FWHM of intense XRD peaks of the as-synthesized ZnS and doped ZnS samples are 1.0 nm and 1.1 nm, respectively. Fig. 3(a) shows the representative TEM image of ZnS sample and Fig. 3(b) shows the corresponding particle size distribution. From the Figs. 3(a) and 3(b), it is seen that the synthesized particles are monodispersed and average particle size for ZnS sample is 1.0 nm which matches quite well those data obtained from XRD measurement.

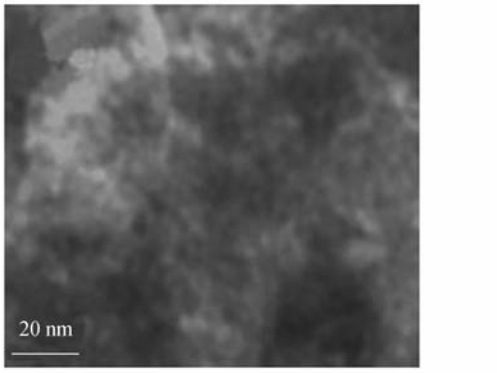

(a) Representative TEM image of ZnS sample

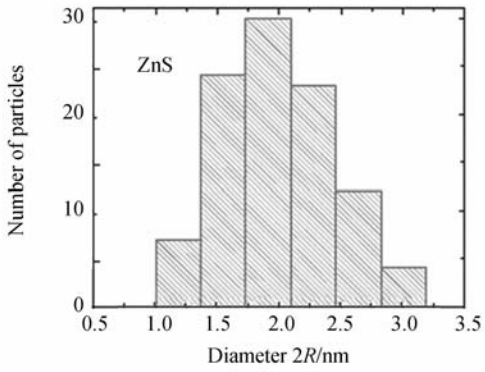

(b) Corresponding particle size distribution

Fig. 3　Representative TEM image and corresponding particle size distribution

The linear optical transmission and photoluminescence (PL) emission characteristics of the used samples dispersed in methanol are shown in Fig. 4. Curves marked as 1 and 2 correspond to linear transmission characteristics of ZnS and doped ZnS samples, whereas curves marked as 3 and 4 indicate their respective PL emission characteristics. The transmission band edge of bulk cubic ZnS is at ~ 334 nm. From the Fig. 4, it is clearly observed that the blue shift of the transmission band edge takes place in both the synthesized samples due to quantum confinement effect, as the particle size of the synthesized QDs are less than that of Bohr Exciton radius of bulk ZnS. Due to confinement of both electrons and holes, the lowest energy optical transition from the valence to conduction band will increase

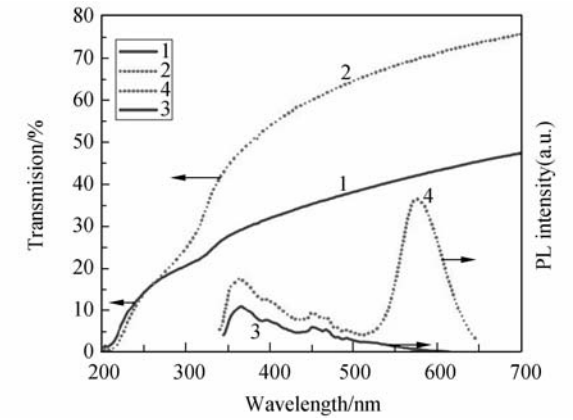

Fig. 4　Linear optical transmission and PL emission characteristics of the samples dispersed in methanol

in energy, effectively increasing the bandgap (E_{gn}) of the QD and we can write:

$$E_{gn}=E_g+\frac{h^2\pi^2}{2\mu R^2}\ . \qquad (2)$$

where, E_g is the bandgap of the bulk semiconductor, h is Planck's constant, R is the radius of the quantum dot, and μ is the reduced mass of the exciton given by $m_e m_h/(m_e+m_h)$. Here, m_e and m_h are masses of the electron and hole, respectively. This model was expanded by Brus[2] to include Coulombic interaction of excitons and the correlation energy and can be written as,

$$E_{gn}=E_g+\frac{h^2\pi^2}{2\mu R^2}-\frac{1.786e^2}{\varepsilon R}+0.284E_R\,, \qquad (3)$$

Here, E_R is the Rydberg (spatial correlation) energy and e is the dielectric constant of the bulk semiconductor. Hence, the UV transmission band-edge of nanoparticles will shift to higher frequency with decreasing diameter particles, with a dependence of $1/R^2$.

Neglecting the polarization term and by substituting $\mu=1.25\times10^{-31}$ kg and $e=8.7$ in Eq. (3), the bandgap of ZnS nanoparticles can be given as,

$$E_{gn}=E_g+\frac{2.7442}{R^2}-\frac{0.2963}{R}\ , \qquad (4)$$

By using linear transmission data and Eq. (4), the calculated average size (radius) of ZnS sample is 1.2 nm which agrees quite well with its value obtained from XRD data analysis and also from the analysis of transmission electron microscope (TEM) micrograph. Photoluminescence emissions from both the samples are also collected and those are also shown in Fig. 4. It is found that the doped ZnS samples show PL emissions in the yellow-green region but undoped ZnS sample exhibits PL emission with a peak at 365 nm lying in the ultraviolet region. However, Mn^{2+} doped ZnS sample emits efficiently with λ_{peak} at 578 nm due to $^4T_1-{}^6A_1$ transition of Mn^{2+}[1-4].

Nonlinear optical properties are measured using the Z-scan technique[7-8]. The Z-scan technique is a simple and straight forward approach for measuring the nonlinear absorption, sign and magnitude of nonlinear refraction of NLO materials. The tightly focused Gaussian beam with TEM00 mode is allowed to pass through the sample and the far field transmittance through the sample is measured by the transmission detector P1, as a function of the position of the sample z with respect to focus. The intensity dependent nonlinear absorption coefficient (β) can be written as[7-9],

$$\alpha=\alpha_0+\beta I\ . \qquad (5)$$

Here, n_0 is linear refractive index at certain wavelength, α_0 is linear absorption coefficient at the certain wavelength in cm^{-1}, β is nonlinear absorption coefficient in cm/W. As the Gaussian beam passes through the material, it experiences phase front and amplitude distortion. Now we assume that the Gaussian beam is traveling along the $+z$ direction. The electric field ξ can be written as,

$$\xi(z,r,t)=\xi_0(t)[w_0/w(z)]\times\exp\{-[r^2/w^2(z)]-[ikr^2/2\times R(z)]\}\times\exp[-i\phi(z,t)]\ . \qquad (6)$$

Where, r is the beam radius at a distance $+z$ and time t, $w(z)=w_0(1+z^2/z_0^2)^{1/2}$, $R(z)=z(1+z_0^2/z^2)$. Here, $w(z)$ and $R(z)$ are the beam radius and radius of curvature of the wave front at a distance $+z$, respectively, and z_0 is the confocal parameter at the incident laser wavelength. The wave vector denoted by $k=2\pi/\lambda$, where λ is

the wavelength of the incident radiation. The temporal envelop and the radially uniform phase variation corresponds the term $\xi_0(t)$ and $\exp[-i\phi(z,t)]$, respectively. By applying the slowly varying approximation we concerned only radial phase changes $\Delta\phi(r)$ and ignore other phase variations[8].

By the above theory it is assumed that, the beam diameter within the sample should not be changed due to nonlinear refraction or due to diffraction. For achieving this, thickness of the sample (L) should be taken as a "thin" *i. e.*, $L<z_0$. In our experimental condition, the sample is regarded as a "thin medium" when $L=0.2$ cm and $z_0=1.348$ cm, so $L<z_0$ condition is easily satisfied. In case of far-field OA Z-scan scheme, the normalized transmittance $T(z)$ in presence of Multiphoton Absorption (MPA) can be written as[16],

$$T_p(z)={}_2F_1\left[\frac{1}{p-1},\frac{1}{p-1},\frac{p}{p-1},-q_{p-1}^{p-1}(z)\right]\&\ , \tag{7}$$

$$q_{p-1}(z)=[(p-1)\beta_{p-1}I_0^{p-1}L_{\text{eff}}^{(p-1)}]^{\frac{1}{p-1}}/(1+z^2/z_0^2)\ , \tag{8}$$

Here, I_0 is the laser beam peak irradiance at the focal plane, $L_{\text{eff}}^{p-1}=[1-\exp\{-(p-1)\alpha_0 L\}]/(p-1)\alpha_0$ is the effective thickness of the sample taking into account of MPA, L is actual thickness of the sample, and ${}_2F_1[\ ]$ is the hypergeometric function.

Fig. 5(a) and 5(b) show the experimental OA Z-scan transmission traces for ZnS and Mn^{2+} doped samples. In these Figs. 5(a) and 5(b) symbols are experimental points and curves are theoretically fitted ones obtained from Eqn. (7) with $p=3,4$, and 5, respectively, for three (TPA), four (FPA) and five (FIPA) photon absorptions. It is seen that experimental Z-scan data deviate significantly from the theoretical curves obtained by considering TPA and FIPA process, whereas curves obtained by using FPA provide the best fits for both the samples. The characteristic absorption band, as shown in

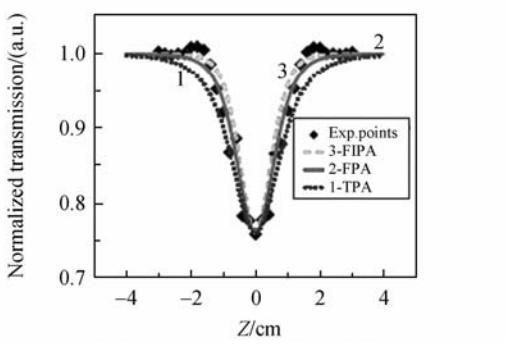

(a) Experimental OA Z-scan transmission traces for ZnS doped sample

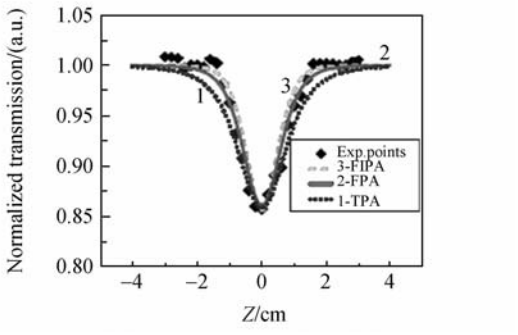

(b) Experimental OA Z-scan transmission traces for Mn^{2+} doped sample

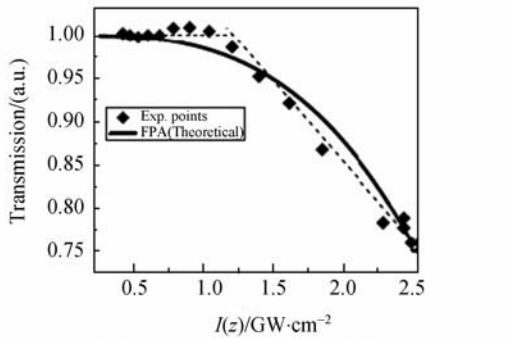

(c) Optical limiting characteristics of ZnS QD colloidal solution in methanol

Fig. 5 Experimental results

Fig. 4, due to the prepared ZnS QDs appeared in 250-340 nm wavelength regions and the bandgaps (E_g) of the used QDs samples are >3.7 eV, while the incident photon energy $E_p=1.17$eV at 1 064 nm. Thus the condition $E_g>3E_p$ is satisfied at 1 064 nm radiations for both the used samples. It clearly eliminates the probability of TPA at 1 064 nm and appears to favor

the process of FPA in present experiment. We have also verified such dominance of FPA by another simple method[7,17]. We have verified dominance of FPA in the used ZnS QDs at 1 064 nm wavelength by using another simple method, which has been first proposed by He *et al*.[17]. By the use of linear fit to the plot of $\ln(1-T_{OA})$ *vs*. $\ln(I)$, where $I=I_o/(1+z^2/z_o^2)$, it is found that the slope of the curve is ~3, (the results are not shown here) which indicates the presence of FPA process. The values of FPA coefficients (β_{FPA}) of 3.1 and 1.8 cm^5/GW^3, respectively for undoped ZnS and Mn^{2+} doped ZnS QDs has been estimated by theoretical fittings to the corresponding experiment data. The FPA cross section (σ_{FPA}) of the ZnS QD has been calculated to be 4.9×10^{-106} $cm^8 \cdot s^3 \cdot photon^{-3}$, by using the relation the $\sigma_{FPA}=[\beta_{FPA}\times(hc/\lambda)^3]/N_o$. Here, N_o is the density of the ZnS QDs in the solution and λ=1 064 nm, the wavelength of the incident radiation. The only available reported value of σ_{FPA} of bulk ZnS is 2.0×10^{-111} $cm^8 \cdot s^3 \cdot photon^{-3}$[18]. Therefore, our measured value of FPA cross section is five orders of magnitude larger than that of bulk ZnS.

The calculated values of nonlinearities are attributed to the semiconductor nanoparticles (ZnS, and Mn^{2+} doped ZnS), since *Z*-scan measurement of the quartz cuvette filled with methanol did not show any such NLO properties. Figure 5(c) shows the optical limiting characteristics of ZnS QD colloidal solution in methanol. From the Fig. 5(c) it is seen that the sample transmits linearly for low value of intensities of the input laser radiation but it transmits nonlinearly for higher laser intensity of the input radiation and the transmission is reduced considerably. As shown in Fig. 5(c), an optical limiting threshold of 1.2 GW/cm^2 has been estimated for the used QD sample at 1 064 nm wavelength.

4 Conclusions

In conclusion, four-photon absorption properties of chemically synthesized ZnS and Mn^{2+} doped ZnS QDs have been reported by *Z*-scan technique by using 10 ns, 1 064 nm Nd : YAG laser radiation with the peak intensity of 2.5 GW/cm^2. The average particle size of the ZnS samples is 1.0 nm which is less than the exciton Bohr radius of 2.2 nm of bulk ZnS. The phase and nanostructures of the samples are characterized by XRD and TEM analyses. Visible PL emission due to $^4T_1 - {}^6A_1$ transition of Mn^{2+} is found in Mn^{2+} doped sample, whereas the undoped sample exhibits PL emission in the ultraviolet region with the peak at 365 nm, which is ascribed to a recombination of electrons at the sulfur vacancy donor level with holes trapped at the zinc vacancy acceptor level. The FPA cross section of the ZnS QD has been calculated to be 4.9×10^{-106} $cm^8 s^3 photon^{-3}$, which is five orders of magnitude larger than that of the available data for bulk ZnS. In a bulk crystal an exciton behaves almost as a harmonic oscillator which does not show any NLO response. Deviation of the electronic excitation from an ideal harmonic oscillator increases as the particle size of crystallite decreases and this causes the enhancement in the nonlinearity. Among other different processes those are reported to be responsible for the induced absorption in semiconductor nanomaterials, four-photon absorption is found to be the basic mechanism in the present experiments with 1 064 nm laser radiation.

In FPA, because of cubic dependence of intensity, it is advantageous for applications, such as in optical limiting. Also materials with multiphoton absorption will provide better resolution in multiphoton spectroscopy due to better spatial localization of the volume probed. The simultaneous presence of large FPA cross section and large luminescence efficiency in the visible region in 2.5% Mn^{2+} doped ZnS QD would render this material as a good candidate, for optical limiting and multiphoton fluorescence imaging applications.

5 Acknowledgments

The author gratefully acknowledged DST (Grant No. SR/FTP/PS-67/2008), Govt. of India for the partial financial support. He is also thankful to Sri M. Chattopadhyay and Sri R. Sarkar of NIT Durgapur, India for their help.

References:

[1] BHARGAVA R N, GALLAGHER D. Optical properties of manganese-doped nanocrystals of ZnS[J]. *Phys. Rev. Lett*, 1994, 72(3): 416-419.

[2] BRUS L E. Quantum crystallites and nonlinear optics[J]. *Appl. Phys. A*, 1991, 53(6): 465-474.

[3] WANG Z L. (*Eds.*). *Handbook of Nanophase and Nanostructured Materials Synthesis*[M]. Beijing: Tsinghua University Press and Kluwer Academic Plenum Publishers, 2002.

[4] SARKAR R, TIWARY C S, KUMBHAKAR P, *et al*.. Yellow-orange light emission from Mn^{2+}-doped ZnS nanoparticles[J]. *Physica E*, 2008, 40(10): 3115-3120.

[5] BANFI G P, DEGIORGIO V, GHIGLIAZZA M, *et al*.. Two-photon absorption in semiconductor nanocrystals[J]. *Phys. Rev. B*, 1994, 50(8): 5699-5702.

[6] MICHALET X, PINAUD F F, BENTOLILA L A, *et al*.. Quantum dots for live cells, in vivo imaging and diagnostics[J]. *Science*, 2005, 307: 538-544.

[7] CHATTAOPADHYAY M, KUMBHAKAR P, TIWARY C S, *et al*.. Multiphoton absorption and refraction in Mn^{2+} doped ZnS quantum dots[J]. *J. Appl. Phys*, 2009, 105(2): 024313.

[8] SHEIK-BAHAE M, HUTCHINGS D C, HAGAN D J, *et al*.. Dispersion of bound electron nonlinear refraction in solids[J]. *IEEE J. Quantum Electron*, 1991, 27(6): 1296-1309.

[9] GANEEV R A. Nonlinear refraction and nonlinear absorption of various media[J]. *J. Opt. A: Pure Appl. Opt*, 2005, 7(12): 717-733.

[10] HE J, SCHOLES G D, ANG Y L, *et al*.. Direct observation of three-photon resonance in water-soluble ZnS quantum dots[J]. *Appl. Phys. Lett*, 2008, 92(13): 1311141.

[11] ZHENG J, ZHANG G, GUO Y, *et al*.. Two-photon absorption properties of Mn-doped ZnS quantum dots[J]. *Chin. Phys. Lett*, 2006, 23(11): 3097.

[12] HE J, QU Y L, LI H P, *et al*.. Three-photon absorption in ZnO and ZnS crystals[J]. *Opt. Exp*, 2005, 13(23): 9235-9247.

[13] HASSAN A R, RAOUF R. Four-photon transitions in semiconductors[J]. *Phys. Stat. Sol. (b)*, 1980, 100(1): 355-360.

[14] YEE J H. Four-photon transition in semiconductors[J]. *Phys. Rev. B*, 1971, 3(2): 355-360.

[15] CULLITY B D. *Elements of X-ray Diffraction*[M]. 2nd ed. Addison-Wesley Company, 1956: 102.

[16] GU B, WANG J, CHEN J, *et al*.. Z-scan theory for material with two-and three-photon absorption[J]. *Opt. Exp*, 2005, 13(23): 9230-9234.

[17] HE J, QU Y L, LI H P, *et al*.. Three-photon absorption in ZnO and ZnS crystals[J]. *Opt. Exp*, 2005, 13(23): 9235-9247.

[18] CATALANO I M, CINGOLANI A, MAFRA A. Four-photon transitions in ZnS[J]. *Solid State Commun*, 1975, 16(9): 1109-1111.

作者简介:

KUMBHAKAR P (1973—), male, was born in Bankura. He received his B. S. degree (Physics) in Burdwan University, 1993; M. S. degree (Physics) in Burdwan University, 1995; Ph. D. degree in Burdwan University, 2003. Now, he is an associate professor, and mainly engaged in research of the area of nanophotonics, nonlinear optics, partial discharge sensor, *etc*. E-mail: nitdgpkumbhakar@yahoo.com & pathik.kumbhakar@phy.nitdgp.ac.in